Cancer Immunology, Immunotherapy (2025) 74:55
https://doi.org/10.1007/s00262-024-03909-w

RESEARCH

CCR5 and IL-12 co-expression in CAR T cells improves antitumor efficacy by reprogramming tumor microenvironment in solid tumors

Yonggui Tian[1,2] · Liubo Zhang[1] · Yu Ping[1] · Zhen Zhang[1] · Chang Yao[1] · Chunyi Shen[1] · Feng Li[1,3] · Chunli Wen[1] · Yi Zhang[1,3,4,5,6]

Received: 20 August 2024 / Accepted: 29 November 2024 / Published online: 3 January 2025

Abstract

Chimeric antigen receptor (CAR) T cell therapy for solid tumors faces significant challenges, including inadequate infiltration, limited proliferation, diminished effector function of CAR T cells, and an immunosuppressive tumor microenvironment (TME). In this study, we utilized The Cancer Genome Atlas database to identify key chemokines (CCL4, CCL5, and CCR5) associated with T cell infiltration across various solid tumor types. The CCL4/CCL5-CCR5 axis emerged as significantly correlated with the presence of T cells within tumors, and enhancing the expression of CCR5 in CAR T cells bolstered their migratory capacity. Furthermore, single-cell immunoprofiling of tumor tissues revealed that macrophages within the TME primarily interact with $CD8^+$ T cells, impeding their tumor response. However, CAR T cells engineered to secrete Interleukin (IL)-12 can counteract macrophage-mediated immunosuppression and augment T cell functionality. To address these obstacles, we employed esophageal carcinoma as a model to develop mesothelin-targeted CAR T cells co-expressing CCR5 and IL-12 (CARTmeso-5-12), subsequently assessing their antitumor capabilities in vitro and in vivo. The CARTmeso-5-12 cells demonstrated enhanced tumor infiltration due to overexpression of CCR5, and IL-12 secretion further amplified CAR T cell efficacy by attenuating the suppressive influence of tumor-infiltrating macrophages, thus improving tumor eradication.

Keywords CAR T cells · CCR5 · IL-12 · TumorMircoenvironment

Introduction

Immunotherapy has played an increasingly vital role in tumor treatment, among which CAR T therapy is one of the most promising therapies. CAR T cells can recognize and kill tumors in a non-major histocompatibility complex-restricted manner by genetically modifying T cells [1]. The CAR structure consists of extracellular single-chain variable fragments (scFv) that recognize tumor-specific antigens, transmembrane domain, and intracellular domain that activates T cell signaling [1, 2]. CAR T cells have brought tremendous and durable responses in the treatment of B-cell hematological malignancies. At present, several CAR T cell products have been approved for treatment of hematological tumors in clinical [3, 4]. Nevertheless, the conversion of CAR T cells to solid tumor therapy confronts various obstacles, which weaken the application of CAR T cells in vivo.

Compared with hematological tumors, the important feature of solid tumors is the presence of tumor microenvironment (TME). CAR T cells need to home and infiltrate into solid tumor tissues to perform their function. And the poor

Yonggui Tian, Liubo Zhang, Yu Ping, Zhen Zhang are contributed equally to this work.

✉ Yi Zhang
yizhang@zzu.edu.cn

1 Biotherapy Center, The First Affiliated Hospital of Zhengzhou University, Zhengzhou 450052, Henan, China

2 Department of Laboratory Medicine, The Third Affiliated Hospital of Zhengzhou University, Zhengzhou, Henan, China

3 State Key Laboratory of Esophageal Cancer Prevention & Treatment, Zhengzhou University, Zhengzhou 450052, Henan, China

4 Tianjian Laboratory of Advanced Biomedical Sciences, Academy of Medical Sciences, Zhengzhou University, Zhengzhou, Henan, China

5 School of Public Health, Zhengzhou University, Zhengzhou, Henan, China

6 School of Life Sciences, Zhengzhou University, Zhengzhou, Henan, China

efficacy of CAR T cells against solid tumors is closely associated with the insufficient infiltration of immune cells in the TME [5, 6]. Improving the migration and accumulation of CAR T cells at tumor sites is a prerequisite for realizing their effector functions. Chemokines and their receptors play a crucial role in mediating the directed migration of immune cells [5, 7]. Many studies have revealed that in order to promote CAR T cells homing to tumor sites, it is a feasible strategy to introduce appropriate chemokine receptors to modify CAR T cells, such as CXCR1, CXCR2, CCR2, or CCR4, etc. [8–10]. Therefore, it is necessary to identify the key chemokine axes in solid tumors for effective genetic modification of CAR T cells to improve their accumulation in tumor tissues. Besides, the immunosuppressive TME is another major barrier, which contains abundant immunosuppressive cells to affect CAR T cell function [11, 12]. The exact immune cells involved in the inhibition of these T cells, however, remain to be elucidated. Among them, tumor-associated macrophages (TAMs) are important immunoregulatory cells that promote tumor immune tolerance, with subpopulations of tumor-suppressing (M1) and tumor-promoting (M2) macrophages [13, 14]. The removal of M2 cells helps to relieve the inhibitory effect on CAR T cells and improve the therapeutic effect [15].

Herein, based on the above scientific issues and related research, we selected single-cell RNA sequencing (scRNA-seq) results from the common and high-incidence lung cancer and esophageal cancer (ESCA) and the cancer genome atlas (TCGA) database to deeply study the problems of immune infiltration and inhibitory TME in solid tumors and seek ways to solve these problems to improve efficacy of CAR T cell. By exploring, we chose to overexpress CCR5 to promote the accumulation of CAR T cells in the tumor site (CARTmeso-CCR5). Introducing IL-12 into CAR T cells remodeled TAMs by inhibiting the expression of M2-related genes and promoting the expression of M1-related genes to reverse the suppressive TME, while enhancing the proliferation and effector function of CAR T cells (CARTmeso-IL12). Finally, to overcome different solid tumor obstacles at once, we designed an enhanced CAR T cell co-expressing CCR5 and IL-12 (CARTmeso-5-12). We found that CARTmeso-5-12 cells improved the ability of infiltrating tumors through CCR5 expression and augmented the function and simultaneously attenuated the inhibitory effect of the TME by adding IL-12, thereby enhancing CAR T cell efficacy.

Materials and methods

Cell lines

The human esophageal cancer cell lines (KYSE-150, KYSE-70, KYSE-510, TE1, EC1, and TE7) and the human embryonic kidney cell line 293 T were purchased from the Cell Bank of the Chinese Academy of Sciences (Shanghai, China). All cell lines were cultured in Dulbecco's Modified Eagle Medium (Sigma-Aldrich, St. Louis, MO, USA) containing 10% fetal bovine serum (FBS, HyClone, Logan, UT, USA), 100 U/mL penicillin, and 100 µg/mL streptomycin without mycoplasma, at the 37 °C humidified incubator with 5% CO_2. The KYSE-510 cells were transfected with CCL5 overexpression lentiviruses (GeneChem, China, GV492/Ubi-MCS-3FLAG-CBh-gcGFP-IRES-Puro) to stably overexpress CCL5 (KYSE-510-CCL5 cells).

Sorting and culture of T cells and macrophages

Peripheral blood mononuclear cells (PBMCs) were isolated from peripheral blood of healthy donors by using density gradient centrifugation. $CD3^+$ T cells and $CD14^+$ cells in PBMCs were positively sorted using human CD3 and CD14 microbeads (Miltenyi Biotec, Bergisch Gladbach, Germany), respectively. $CD3^+$ T cells were cultured in RPMI-1640 medium (Sigma-Aldrich) with 200 U/mL IL-2. $CD14^+$ monocytes were induced for 7 days in RPMI-1640 medium with 20 ng/mL M-CSF (PeproTech, Rocky Hill, NJ, USA) and then incubated for 2 days with IL-4 (PeproTech) to polarize macrophages into M2. The induced M2 cells were cultured for 3 days with IL-12 protein or CAR T cell supernatant incubated with tumor cells for 24 h to detect phenotypic and polarization-related genes of macrophages.

Lentivirus and CAR T cell generation

Meso-CAR consisted of a scFv, the costimulatory domains of CD28 and 4-1BB, and CD3-zeta domains. CD19-CAR was used as the control group in our study. Human CCR5 (CARmeso-CCR5) or IL-12 (CARmeso-IL-12) genes connected with meso-CAR through P2A linker, respectively. CARmeso-CCR5-IL-12 contained the CCR5 gene initiated by CMV promoter, and the EF1a-promoted the structure, which meso-CAR was linked to IL-12 via P2A. These sequences were synthesized by Sangon Biotech (Shanghai, China) and cloned into the lentiviral vector pCDH-EF1 (System Biosciences, Palo Alto, CA, USA) expressing green fluorescent protein (GFP). The constructed plasmids were transfected into 293 T cells by jetPRIME transfection reagent (polyplus-transfection, France) to generate lentiviral particles, and the virus supernatant was added into activated T cells. Subsequently, transduction efficiency GFP and expression of CCR5 and IL-12 were detected by flow cytometry.

Primary tumor samples

Tissue samples were collected from 38 patients with esophageal cancer (ESCA) treated surgically in the First Affiliated Hospital of Zhengzhou University. Each patient signed a written informed consent form for participation, which was reviewed and approved by the Ethics Committee of the First Affiliated Hospital of Zhengzhou University. These patients had not received chemotherapy, radiotherapy, or other therapy prior to the surgical treatment. Fresh tumor tissues and paired adjacent normal tissues (at least 5 cm away from the tumor site) were obtained from the patients.

TCGA multi-cancer data analysis

The tumor mRNA data of TCGA database were downloaded from UCSC Xena platform (https://xenabrowser.net/datapages/). RTCGA R-packet was used to obtain the genome expression data of six solid tumors in TCGA. Meta-analysis of correlation was carried out by using metafor to generate forest map. The phenotypic characteristic data of each immune subgroup were downloaded from UCSC Xena. According to the phenotypic data, the immune cells of the six cancers obtained were evaluated by GSVA package, and the median expression of chemokine CCL5 was calculated. The expression of CCL5 was more than or equal to the median, which was defined as the high expression group, and less than the median was defined as the low expression group, and the heat map was used to show the immune infiltration.

Online analysis of public database

The correlation between CCL4/CCL5 and $CD8^+$ T cell infiltration was analyzed online using the Tumor IMmune Estimation Resource (TIMER, http://timer.cistrome.org). The expression levels of CCL4 and CCL5 in tumor tissues were obtained from the Gene Expression Profiling Interactive Analysis database (GEPIA, http://gepia.cancer-pku.cn). In addition, the correlation between IL-12 and the expression of CD8A, CD69, IFNG, and GZMB genes in ESCA can be acquired from cBioPortal (https://www.cbioportal.org/).

ScRNA-seq data dimensionality reduction and cluster analysis

The data of ESCA scRNA-seq were obtained from the Gene Expression Omnibus database (GEO), and the accession number was GSE145370 (https://www.ncbi.nlm.nih.gov/geo/). The scRNA-seq data for lung cancer were downloaded from EMBL-EBI database (www.EBI.ac.uk/ArrayExpress) under the accession numbers E-MATB-6149 and E-MATB-6653. We normalized and standardized the expression values of each cell. And the cells that passed the quality control were included in the subsequent analysis. We used the RunPCA function for principal component analysis (PCA) and determined the optimal number of principal components (dim = 15) through the ElbowPlot function. Next, we used Seurat package to perform cluster analysis of single-cell data. In order to display the data after PCA dimension reduction in three-dimensional or two-dimensional space more intuitively, we further used the dimensionality reduction method of uniform manifold approximation and projection (UMAP) to visualize the data, so as to better explore the law and essence reflected behind the single-cell data.

Proportion analysis of various immune cell subsets

We annotated various cell types according to the reported marker genes and analyzed the abundance of various immune cells. We used the ggplot package to count and calculate the proportion of these cell subsets in tumor samples and plotted a stacked histogram.

Immune cell interaction analysis

We quantified and evaluated cellular interactions through the binding of immune checkpoints. The Pearson correlation coefficient was calculated to evaluate the co-expression level of a single paired ligand-receptor, and the ComplexHeatmap package was used to generate a heat map to show the correlation of the ligand-receptors expression in each interacting cell.

Quantitative real-time PCR (qRT-PCR)

Total cellular RNA from tissue samples and macrophages was extracted using TRIzol (Invitrogen, Carlsbad, CA, USA). cDNA was prepared with the Primescript RT Reagent Kit (TakaRa, Dalian, China). QRT-PCR analysis was performed using the SYBR Green Master Mix (Roche, Basel, Switzerland) in PCR System (Agilent Stratagene, Santa Clara, CA). And the data were analyzed by comparative Ct quantification. Glyceraldehyde-3-phosphate dehydrogenase (GAPDH) was used as internal reference gene. The primers are listed in Table 1.

Mesothelin expression analysis

To study mesothelin expression in different ESCA cell lines, digested tumor cells were washed with PBS and, respectively, labeled with isotype antibody (Miltenyi Biotec, Order no. 130–113-438) and mesothelin antibody (Miltenyi Biotec, Order no. 130–118-168). The samples were detected by FACS Canto II flow cytometer (BD Biosciences, Franklin Lakes, NJ, USA).

Table 1 Primers for qRT-PCR

Genes	Primers (5′-3′)
GAPDH	Forward-GGAGCCAAAAGGGTCATCACTC
	Reverse- GAGGGGCCATCCACAGTCTTCT
CCL4	Forward-TGCTAGTAGCTGCCTTCTGC
	Reverse-TTCACTGGGATCAGCACAGAC
CCL5	Forward-CCGCCAAGTGTGTGCCAACC
	Reverse-CCTTCAAGGAGCGGGTGGGG
CD163	Forward-ACTTGAAGACTCTGGATCTGCT
	Reverse-CTGGTGACAAAACAGGCACTG
MRC1	Forward-GGGTTGCTATCACTCTCTATGC
	Reverse-TTTCTTGTCTGTTGCCGTAGTT
TGF-b	Forward-GCCAGAGTGGTTATCTTTTGATG
	Reverse-AGTGTGTTATCCCTGCTGTCAC
IL-6	Forward-ACTCACCTCTTCAGAACGAATTG
	Reverse-CCATCTTTGGAAGGTTCAGGTTG
TNF-a	Forward-CTGTAGCCCATGTTGTAGCAAAC
	Reverse-GCTGGTTATCTCTCAGCTCCAC
ARG1	Forward-GTCTGTGGGAAAAGCAAGCG
	Reverse-CACCAGGCTGATTCTTCCGT
IL-10	Forward-TTTAAGGGTTACCTGGGTTGC
	Reverse-TTGATGTCTGGGTCTTGGTTC
IL-1b	Forward-ATGATGGCTTATTACAGTGGCAA
	Reverse-GTCGGAGATTCGTAGCTGGA
NOS2	Forward-TTCAGTATCACAACCTCAGCAAG
	Reverse-TGGACCTGCAAGTTAAAATCCC

Flow cytometry

The collected cells were washed with PBS and incubated with fluorescence-conjugated antibodies for 15 min at 4 °C in the dark to conduct surface marker staining. To examine intracellular staining, the cells were co-cultured with tumor cells for 24 h. Cell samples were stained for intracellular cytokines after surface staining, fixation, and permeabilization. The antibodies used were purchased from BioLegend (CCR5, Cat. 359,122; IL-12, Cat. 501,807; Ki67, Cat. 350,514; IFN-g, Cat. 986,702; Granzyme B, Cat. 372,212). FACSCanto II flow cytometer was used to detect the phenotype and function of cells.

Cytotoxicity assay

CAR T cells were incubated with tumor cells at different effector-to-target (E/T) ratios for 6 h. The tumor cells were collected and stained with annexin V (BioLegend, Cat. 640,920) in Annexin-V Binding Buffer for 15 min at 4 °C in the dark. Propidium iodide (BioLegend, Cat. 421,301) was added before testing, and then the lysis rate was measured by flow cytometer.

Transwell assay

Transwell assays were performed in 24-well plates with 5-μm Transwell chambers (Corning Inc., Corning, NY, USA). CAR T cells (5×10^5 cells per well) were placed in the upper chamber. Recombinant human CCL4 and CCL5 proteins (PeproTech) or culture supernatants of KYSE-510-CCL5 cells were added to the lower chamber. Transwell plates were incubated for 3 h at 37 °C. The cells in the bottom wells were collected and counted by Accuri C6 flow cytometry.

Enzyme-linked immunosorbent assay (ELISA)

CAR T cells were incubated with tumor cells for 24 h, and the supernatants were collected. The secretion of IL-12 was probed according to ELISA kit instructions (BioLegend). The protein concentrations were calculated by measuring the optical density value at 450 nm. The culture supernatants of KYSE-510 and KYSE-510-CCL5 cells were harvested and detected CCL5 production using the LEGENDplex™ Human Proinflammatory Chemokine Panel (BioLegend, Cat. No. 740003).

Imaging Flow Cytometry

The CAR T cells supernatant-treated macrophages were harvested and stained with fluorescein-conjugated antibodies CD14 (BioLegend, Cat. 982,506), CD163 (BioLegend, Cat. 326,506), and CD86 (BioLegend, Cat. 374,210). DAPI (4’,6-diamidino-2-phenylindole; Thermo Fisher Scientific, Waltham, MA, USA) was used to label cell nucleus. Then the samples were tested using the ImageStream MKII system (Amnis, Germany).

Immunofluorescence (IF)

The collected macrophages were washed with pre-cooled phosphate-buffered saline (PBS) and fixed with 4% paraformaldehyde. Cells were then incubated with CD163 antibody (Abcam, UK, ab87099, 1:200) overnight at 4 °C. Subsequently, the cells were stained with Alexa Fluor 488-conjugated goat anti-rabbit IgG, used as the secondary antibody, at room temperature for 1 h. And nuclei were counterstained with DAPI. The samples were observed and photographed under fluorescence microscope (Leica, Wetzlar, Germany).

In vivo studies

Five-week-old female immunodeficient mice (NOD/SCID) were purchased from Vital River Laboratory Animal Technology Company (Beijing, China) and reared at the Henan

Key Laboratory for Pharmacology of Liver Diseases. All animal experiments were approved by the Animal Care and Ethics Committee of the First Affiliated Hospital of Zhengzhou University and conducted in accordance with the animal experiment guidelines. Mice were subcutaneously injected with 2×10^6 cells, which KYSE-510 expressing luciferase and CCL5, and M2 cells were mixed in 1: 1 ratio, as previously reported [16, 17]. Mice were randomly divided into four groups after tumor nodules appeared (5 mice/group), and 5×10^6 CAR T cells were infused intravenously on day 7. To evaluate the tumor infiltration in vivo, tumor tissues were collected and embedded in paraffin for immunohistochemistry after 7 days of CAR T cell infusion. Besides, tumor growth was monitored by detecting tumor bioluminescence or measuring tumor diameter with a caliper (tumor volume = [(length × (width) [2]]/2). Xenogen IVIS-200 Spectrum camera and Living Image version 4.4 (Caliper Life Sciences, Waltham, MA, USA) were used for image acquisition and analysis. Once the tumor volume reached 1200 mm^3, or there were signs of discomfort, the mice were euthanized.

Immunohistochemistry (IHC)

Paraffin-embedded tissue sections were first baked, deparaffinized, and subjected to antigen retrieval. Endogenous oxidase was then inactivated by incubation with 3% hydrogen peroxide and blocked with 5% goat serum. And the sections were stained with anti-CD3 (Abcam, ab16669, 1:150) or anti-CD163 antibody (Abcam, ab28364, 1 mg/mL) overnight. The next day, biotinylated secondary antibody was used for staining. After staining with DAB solution, the sections were counterstained with hematoxylin and sealed with neutral resin. The sections were recorded and photographed under the microscope. Five fields of each slice were randomly selected based on the frequency of positive cells and staining intensity for evaluation and statistics. The intensity was scored as follows: 0, negative; 1, light yellow; 2, brown; and 3, deep brown. The frequency of positive cells was defined as follows:0, 0%; 1, 1% to 25%; 2, 26% to 50%; 3, 51% to 75%; and 4, greater than 75%. The two integral results were added to determine the grade of slice dyeing.

Statistical Analysis

All in vitro experiments were repeated at least three times, and five mice were studied in each group in vivo. Statistical results were analyzed using GraphPad Prism 8.0 (GraphPad Software, La Jolla, CA). The t-test and ANOVA (Turkey) were used to perform statistical difference analysis. The survival curve was determined by the log-rank test. All the data were presented as the mean ± SEM. Statistical differences were set at $P < 0.05$, and $P > 0.05$ was considered not significant (ns).

Results

CCL4 and CCL5 are important chemokines for T cell infiltration in solid tumors

Immune cell infiltration within the TME profoundly influences patient prognosis, underscoring the necessity of identifying chemokines attracting T cells into tumor tissues. Utilizing the TCGA database, we investigated the correlation between various chemokines and CD8A expression across multiple solid tumor types at the transcriptional level, revealing that CCL5 was the most robust and consistent positive correlation with CD8A expression, whereas other chemokines lacked similar associations (Fig. 1A, B). Subsequently, we stratified the TCGA tumor samples into groups based on CCL5 expression, examining their impact on the infiltration of immune cell subsets. A heat map demonstrated that the high-expression group of CCL5 had a superior capacity to attract $CD8^+$ T cells, natural killer cells, cytotoxic lymphocytes, and dendritic cells, while low-expression group exhibited a diminished immune presence (Fig. 1C). These findings underscore that tumors with elevated CCL5 levels typically harbor extensive immune cell infiltration.

Furthermore, we validated a highly consistent positive correlation between CCL5 expression and $CD8^+$ T cell infiltration across various solid tumor tissues using the TIMER platform (Fig. 1D). Additionally, CCL4, which shares the same receptor as CCL5, showed a significant relationship with $CD8^+$ T cell infiltration as well (Fig. S1A). This pattern suggests that both CCL4 and CCL5 are integral to T cell recruitment within solid tumors. Our analysis of the expression levels of CCL4 and CCL5 in tumor versus adjacent non-tumor tissues revealed higher levels of these chemokines in tumor tissues (Fig. 1E and S1B). Using tissue samples of ESCA patients, we further confirmed the elevated expression of CCL4 and CCL5 in tumor tissues relative to adjacent non-tumor tissues (Fig. 1F and S1C). Collectively, this evidence indicates that CCL4 and CCL5 create a concentration gradient within tumor tissues, which favors T cell recruitment to tumor sites.

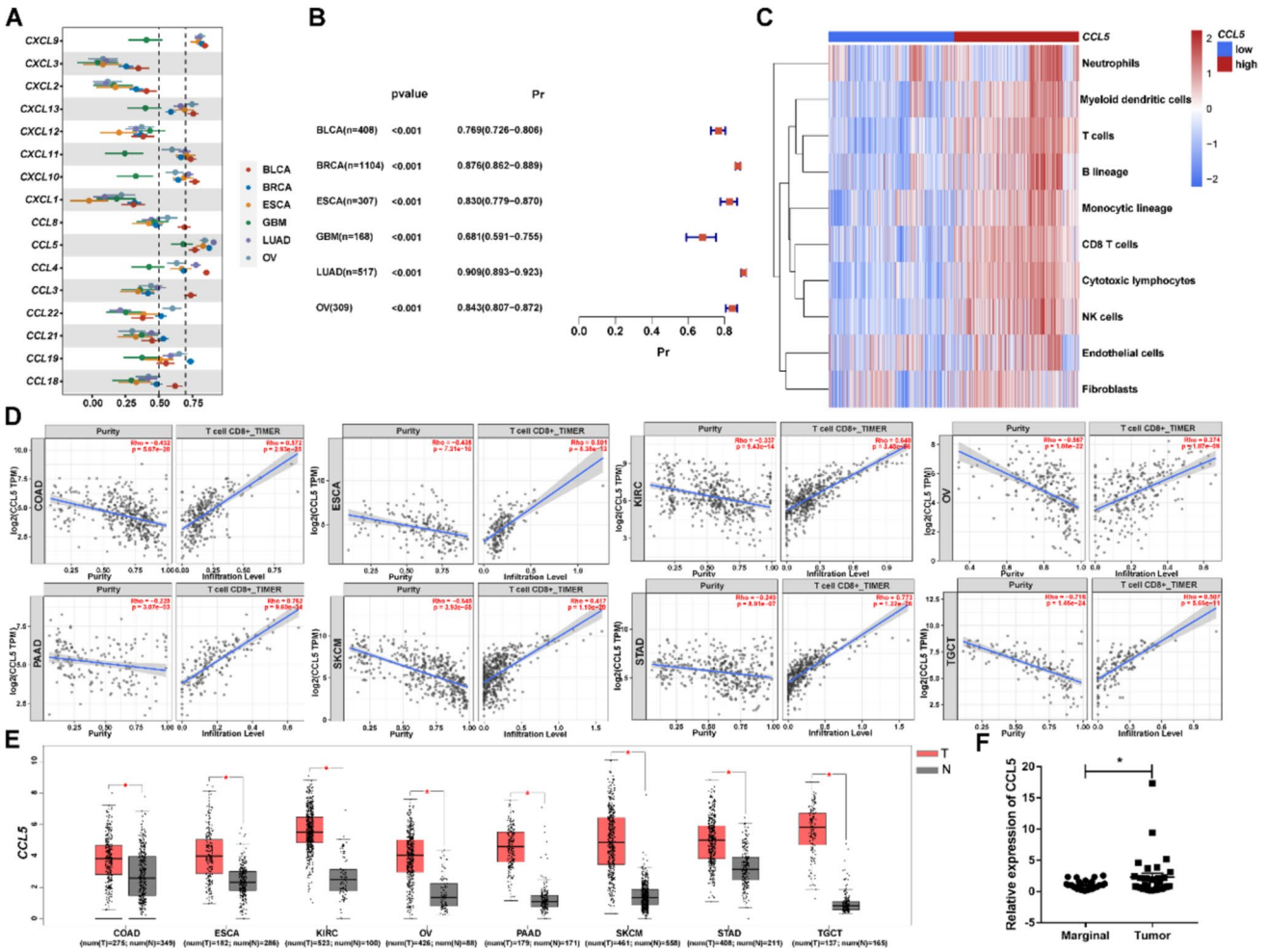

Fig. 1 Chemokine CCL5 was associated with T cell infiltration in solid tumors. **A** Forest plot of the correlation between different chemokines and CD8A expression in TCGA database. **B** The relativity between CCL5 and CD8A expression in various solid tumors was demonstrated, where Pr represents Pearson correlation. **C** The heat map showed the gene signature scores of each immune subgroup in the tumor tissues of the high or low CCL5 expression group. **D** The relationship between CCL5 and $CD8^+$ T cell infiltration in eight solid tumors was analyzed by TIMER database. Spearman's correlation analysis is used for statistical analysis. **E** Expression analysis of CCL5 in neoplastic and non-neoplastic tissues from different solid tumors using GEPIA data. $*p < 0.05$, Student's t test. **F** The expression of CCL5 in ESCA tumor and marginal tissues was analyzed by qRT-PCR (n = 31). $*p < 0.05$, Student's t test. BLCA, Bladder Cancer; BRCA, Breast Cancer; ESCA, Esophageal Cancer; GBM, Glioblastoma; LUAD, Lung Adenocarcinoma; OV, Ovarian Cancer; COAD, Colon Cancer; KIRC, Kidney Clear Cell Carcinoma; PAAD, Pancreatic Cancer; SKCM, Melanoma; STAD, Stomach Cancer; TGCT, Testicular Cancer; T, Tumor; N, Normal

Enhanced migration of CAR T cells via CCR5 incorporation

CCR5, a receptor with high-affinity binding for CCL4 and CCL5, mediates chemotaxis. Previous studies have identified positive correlation between the abundance of CCL4 and CCL5 with $CCR5^+CD8^+$ cytotoxic T lymphocytes and patient survival [18]. To enhance CAR T cell migration, the CAR construct targeting mesothelin was engineered to include CCR5 via the self-shearing peptide P2A (CARTmeso-CCR5). CD19-targeted CAR T (CART19) cells and mesothelin-specific CAR T (CARTmeso) cells served as controls (Fig. S2A). Following plasmid transduction, a marked increase in CCR5 expression was observed in CARTmeso-CCR5 cells compared to controls (Fig. S2B, C). Subsequently, we employed KYSE-510 and KYSE-150 cells, which express mesothelin at high and low levels, respectively, to evaluate the CAR T cells' cytolytic activity (Fig. S2D). Both CARTmeso and CARTmeso-CCR5 cells demonstrated potent and equivalent cytotoxicity (Fig. S2E). Transwell assay was utilized to assess the influence of CCR5 on CAR T cell chemotactic response, introducing medium containing CCL4 and CCL5 or

supernatant from CCL5-overexpressing KYSE-510 cells (KYSE-510-CCL5) as attractants. The results showed that CARTmeso-CCR5 cells possessed significantly superior migratory capacity relative to CART19 and CARTmeso cells (Fig. S2F–H). In summary, the addition of CCR5 to CAR T cells significantly bolsters their migratory ability, without compromising cytotoxic function.

IL-12 as a potential modulator of the immunosuppressive tumor microenvironment

The TME of solid tumors not only hampers T cell function, but also contributes significantly to poor outcomes in cancer patients. We analyzed the immune profiles of the TME using scRNA-seq datasets from ESCA and lung cancer patients with high incidence and mortality rates [19, 20]. For ESCA, scRNA-seq was conducted on $CD45^+$ immune cells from seven samples of fresh tumors. And the lung cancer dataset comprised eight samples of untreated tumors, which tissues were digested to a single-cell suspension and subjected to scRNA-seq. (Fig. 2A). UMAP analysis of the scRNA-seq data identified cell clusters (Fig. 2B). We noticed a predominance of $CD8^+$ T cells within the tumor-infiltrating immune populations, consistent with the literature (Fig. 2C). Remarkably, M2 macrophages were stable presence across patient samples, maintaining a significant abundance (Fig. 2C). This finding highlights M2 macrophages as key inhibitory components within the TME. Investigating interactions between TAMs and T cells revealed a dominant engagement of TAMs with $CD8^+$ T cells. Despite the identification of a negative co-stimulatory pathway between TAMs and NK cells, the

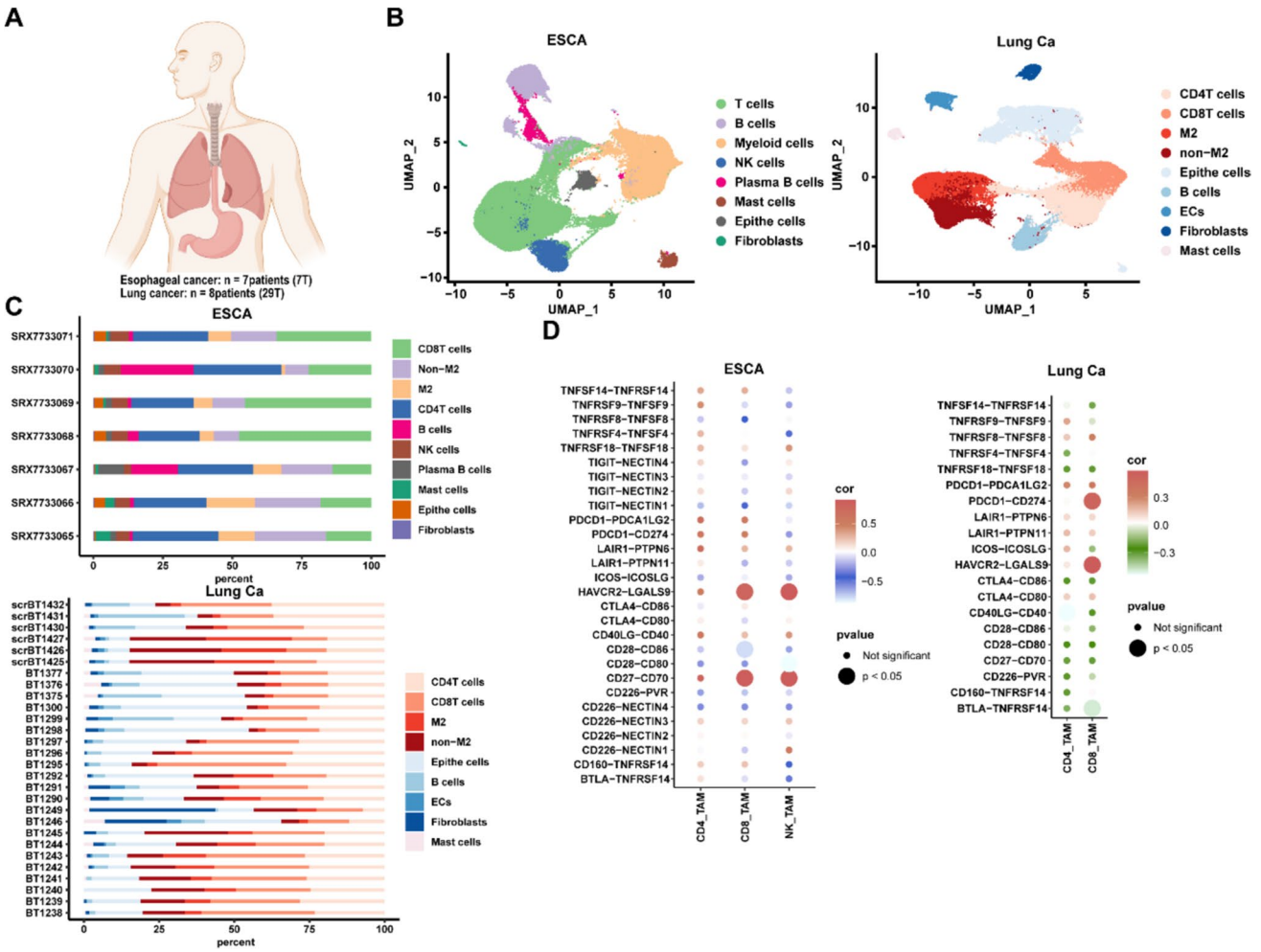

Fig. 2 TAMs were the main inhibitory immune cells in TME. **A** ScRNA-seq data originated from 7 tumor tissue samples collected from 7 ESCA patients, as well as 29 tumor tissue samples from 8 lung cancer patients. **B** The UMAP map of single cell in samples. ESCA samples showed 8 immune cell clusters, and 9 cell clusters were identified in lung cancer tissues. **C** The stack diagram of different immune cell subsets identified by scRNA-seq in tumor tissues. **D** The cell interaction between tumor-infiltrating antitumor cell subsets and TAMs was evaluated by immune checkpoint ligand-receptor binding. Cor indicates Pearson correlation coefficient. T, Tumor; ESCA, Esophageal Cancer; Lung Ca, Lung Cancer; ECs, Endothelial cells

low proportion of NK cells in ESCA and their undetectable presence in lung cancer suggest that NK cells may not play a primary role. The immune checkpoint interaction scores between TAMs and $CD8^+$ T cells reveal that in lung cancer, two inhibitory pathways (HAVCR2-LGALS9 and PDCD1-CD274) are significantly involved, while in ESCA, one negative co-stimulatory pathway (HAVCR2-LGALS9) and one positive co-stimulatory pathway (CD27-CD70) are implicated (Fig. 2D). This suggests that compared to co-stimulatory checkpoint interactions, co-inhibitory checkpoint interactions are more prevalent, indicating an inhibitory effect of TAMs on $CD8^+$ T cell activity (Fig. 2D). Thus, TAMs appear to restrict the antitumor response by dampening $CD8^+$ T cell efficacy, indicating that T cell responses can be enhanced by modulating TAMs.

IL-12 is reported to intensify T cell-mediated tumor immunity and reprogram M2 macrophages into pro-inflammatory M1 phenotype [21, 22]. Utilizing the ESCA dataset from cBioPortal, we noted the positive correlation between IL-12 and genes related to T cell function (Fig. S3A). Examining the polarization effects of IL-12 on macrophages, we observed that IL-12 treatment increased the proportion and gene expression of $CD14^+CD86^+$ M1 macrophages (TNFA and IL6), while $CD14^+CD163^+$ M2 macrophages (MRC1, CD163, and TGFB) diminished (Fig. S3B, C).

IL-12 promotes enhanced functionality in CAR T cells and influences macrophage polarization

To mitigate the suppressive effects, the IL-12 gene was integrated into the mesothelin-targeted CAR construct (Fig. S4A). The engineered CAR T cells, CARTmeso-IL12, demonstrated effective IL-12 expression (Fig. S4B, C). Subsequent functional analysis revealed that CARTmeso-IL12 cells exhibited enhanced capability to lyse tumor cells (Fig. S4D). Assessment of IL-12 concentration in the culture supernatants of CAR T cells confirmed elevated IL-12 levels in CARTmeso-IL12 samples (Fig. S4E). Furthermore, when M2 macrophages were treated with CAR T cell culture supernatants, it was observed that only supernatants from CARTmeso-IL12 cells induced polarization toward M1 phenotype (Fig. S4F, G). These results indicate that CARTmeso-IL12 cells possess superior cytotoxic properties and the ability to affect macrophage polarization.

Enhancing CAR T Cell function through CCR5 and IL-12 overexpression

To recruit more CAR T cells to tumor sites, boost their antitumor efficacy, and counteract the immunosuppressive TME, we engineered a novel CAR construct that concurrently expressed CCR5 and IL-12 (Fig. 3A). Using the CMV and EF1α promoter elements, coupled with 2A peptides, we ensured the simultaneous and stable expression of CAR, CCR5, and IL-12 in CARTmeso-5-12 cells (Fig. 3A-D). CARTmeso-5-12 cells exhibited exceptional proliferation, enhanced cytotoxicity, and increased production of functional molecules compared to other groups (Fig. 3E-G). However, in comparison to CARTmeso, CARTmeso-5-12 demonstrated no notable alterations in its memory phenotype (Fig. S5). Furthermore, the inclusion of CCR5 improved the migratory response of CARTmeso-5-12 to chemokines CCL4 and CCL5 (Fig. 3H). Hence, our results confirm that CAR T cells overexpressing CCR5 and IL-12 possess augmented capabilities to perform their intended functions.

Polarization of macrophages by CARTmeso-5-12 cells

To assess whether CARTmeso-5-12 cells could polarize macrophages, we utilized their supernatants to culture M2 macrophages and subsequently conducted phenotypic and gene expression analyses. Substantial IL-12 secretion was detected in the supernatants from CARTmeso-5-12 (Fig. 4A). Using imaging flow cytometry and flow cytometry, we observed that IL-12 incorporation resulted in increased CD86 expression and decreased CD163 expression (Fig. 4B, C). The immunofluorescence analyses corroborated these findings (Fig. 4D). Macrophage-related gene detection showed the reduction in M2-associated gene expression and the increase in the expression of M1 genes, such as TNF-α, IL-1β, and NOS2, following co-incubation with CARTmeso-5-12 supernatants (Fig. 4E). Collectively, these results indicate that CARTmeso-5-12 cells can polarize macrophages, and have the potential to modulate the inhibitory TME.

IL-12 and CCR5 expression in CAR T cells promotes immune infiltration and modulation of macrophages in vivo

To assess the in vivo efficacy of CAR T cells, we established a mouse model following established protocols, which combined KYSE-510-CCL5 cells with M2 macrophages and injected subcutaneously into mice [16, 17]. After tumor establishment, the sorted CAR T cells were administered intravenously. The tumor specimens were harvested for examination and analysis after 7 days (Fig. 5A). Histopathological evaluation from mice receiving CARTmeso-5-12 cells revealed a substantial increase in T cell infiltration compared to traditional the CAR T cell therapy (Fig. 5B, C). Furthermore, CD163-positive M2 macrophages percentage decreased significantly in CARTmeso-5-12 group (Fig. 5D, E). These findings indicate that CARTmeso-5-12 cells can

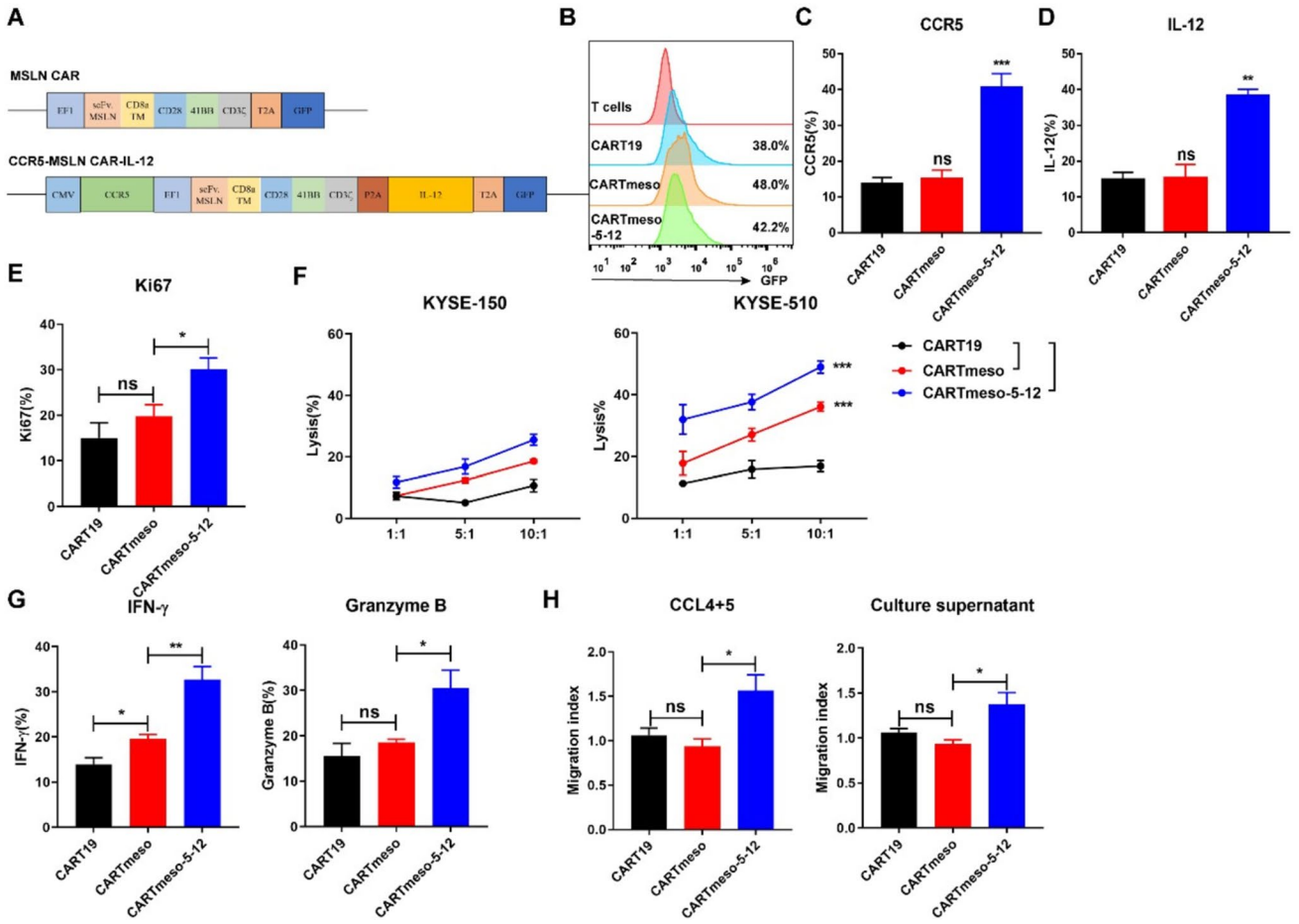

Fig. 3 Overexpression of CCR5 and IL-12 could enhance the function of CAR T cells. **A** Structures of CAR used. **B** The evaluation of transduction efficiency in CAR T cells by flow cytometry. **C**–**E** The expression of CCR5, IL-12 (**C**, **D**), and Ki67 (**E**) in CAR T cells was analyzed by flow cytometry. ns, not significant, $*p<0.05$, $**p<0.01$, $***P<0.001$, one-way ANOVA. **F** CAR T cells were co-incubated with target cells at varying E/T ratios for 6 h. Cell lysis was tested using flow cytometry. $***P<0.001$, two-way ANOVA. **G** CAR T cells were co-cultured with KYSE-510 cells at a 1:1 E:T ratio for 24 h, to determine the expression of CAR T cell effector molecules using flow cytometry. ns, not significant, $*p<0.05$, $**p<0.01$, one-way ANOVA. **H** Transwell was used to evaluate the migration ability of CAR T cells induced by CCL4 and CCL5 proteins or tumor cell supernatants. ns, not significant, $*p<0.05$, one-way ANOVA. All data are represented as mean ± SEM

more effectively infiltrate tumor sites and mitigate the presence of M2 macrophages.

Enhanced tumor suppression by CARTmeso-5-12 Cells in a xenograft model

In a xenograft mouse model, equal parts of macrophages and tumor cells were co-injected subcutaneously. Mice were then treated intravenously with PBS, CART19, CARTmeso, or CARTmeso-5-12 cells after 7 days (Fig. 6A). Subsequent monitoring revealed no significant differences in food consumption or body weight across the groups. Tumor progression was quantified weekly using bioluminescence imaging. Tumors in mice treated with PBS, CART19, and CARTmeso showed exponential growth, whereas growth was substantially slower in tumors from the CARTmeso-5-12 group (Fig. 6B, C). This group also exhibited a significant extension in survival compared to controls (Fig. 6D). Collectively, these results demonstrate the enhanced antitumor capability of CARTmeso-5-12 cells in vivo.

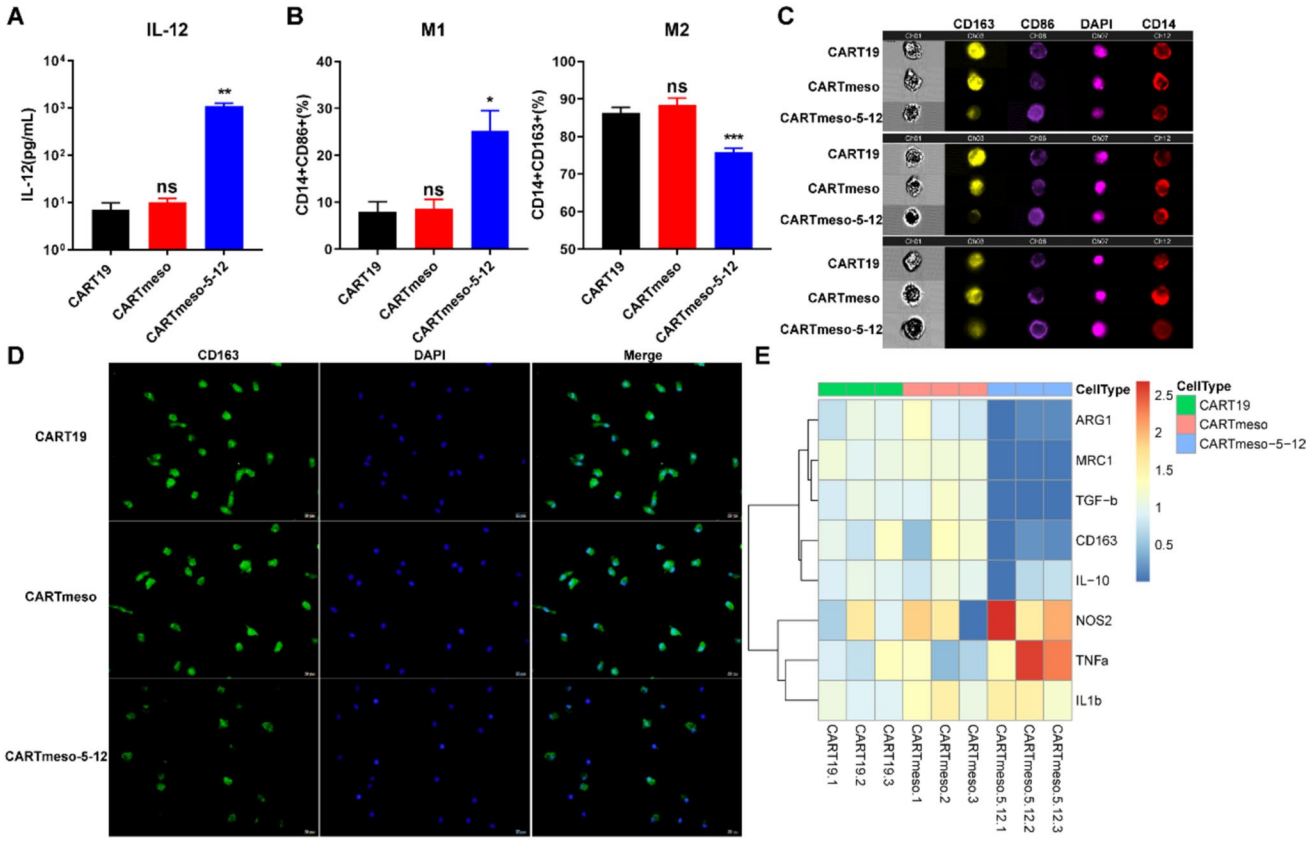

Fig. 4 CARTmeso-5-12 cells showed the capacity of polarizing macrophages. **A** The secretion of IL-12 in CAR T cells. M2 macrophages were incubated with CAR T cell supernatant for 3 days to detect macrophage phenotype and related gene expression. **B** The proportion of M1 and M2 macrophages was detected by flow cytometry. **C** Macrophages were stained with CD86, CD163, and CD14 antibody and checked on image flow cytometer. **D** Immunofluorescence detection of M2 macrophage phenotype CD163. **E** Expression of TNF-a, IL-1b, NOS2, MRC1, CD163, ARG1, IL-10, and TGF-b in macrophages by qRT-PCR. All data are represented as mean ± SEM. one-way ANOVA is used for statistical analysis. ns, not significant, $*p<0.05$, $**p<0.01$, $***P<0.001$

Discussion

The effective killing of CAR T cells against solid tumors is constrained by various reasons. The impaired trafficking of intravenous CAR T cells into the tumors results in insufficient tumor infiltration. Even if they successfully infiltrate solid tumors, CAR T cells must still address their inherent functional challenges, specifically the suppression of their anti-tumor activity by immune checkpoints such as PDL1 and TIM3 [23, 24], while also grappling with the hostile (TME) populated by numerous inhibitory cells, including tumor-associated macrophages (TAMs), myeloid-derived suppressor cells, and regulatory T cells [12, 25, 26]. For these obstacles, researchers are energetically exploring solutions. Overexpression of chemokine receptors on CAR-T cells increases their localization to tumor sites [8, 10, 27]. Additionally, equipping CAR T cells to secrete pro-inflammatory cytokines improves persistence and activity of CAR T cells [28–31]. Remodeling TME relieves CAR T cell suppression and enhances antitumor immune responses [32–34]. Nevertheless, more studies only focused on addressing one barrier, while the other issues still affect the efficacy of CAR T cells. Hence, we modified CAR T cells to overcome various restrictive factors of solid tumors.

In this study, we first used the TCGA database to screen the key chemokines related to T cell infiltration in solid tumors. Only CCL5 showed a highly consistent positive correlation with CD8A expression in different tumor tissues, and the immune infiltration increased in solid tumors with high expression of CCL5, suggesting that CCL5 has the potential to recruit T cells. Moreover, we discovered that CCL4 with the same receptor as CCL5 was strongly and positively associated with the accumulation of $CD8^+$ T cells in tumor tissues, indicating that the CCL4/CCL5-CCR5 axis is closely associated with the immune infiltration. Most importantly, CCL4/CCL5 was highly expressed in various tumor tissues compared with para-cancerous tissues, suggesting that tumor tissues have the concentration gradient of CCL4/CCL5 to recruit cells expressing their receptor

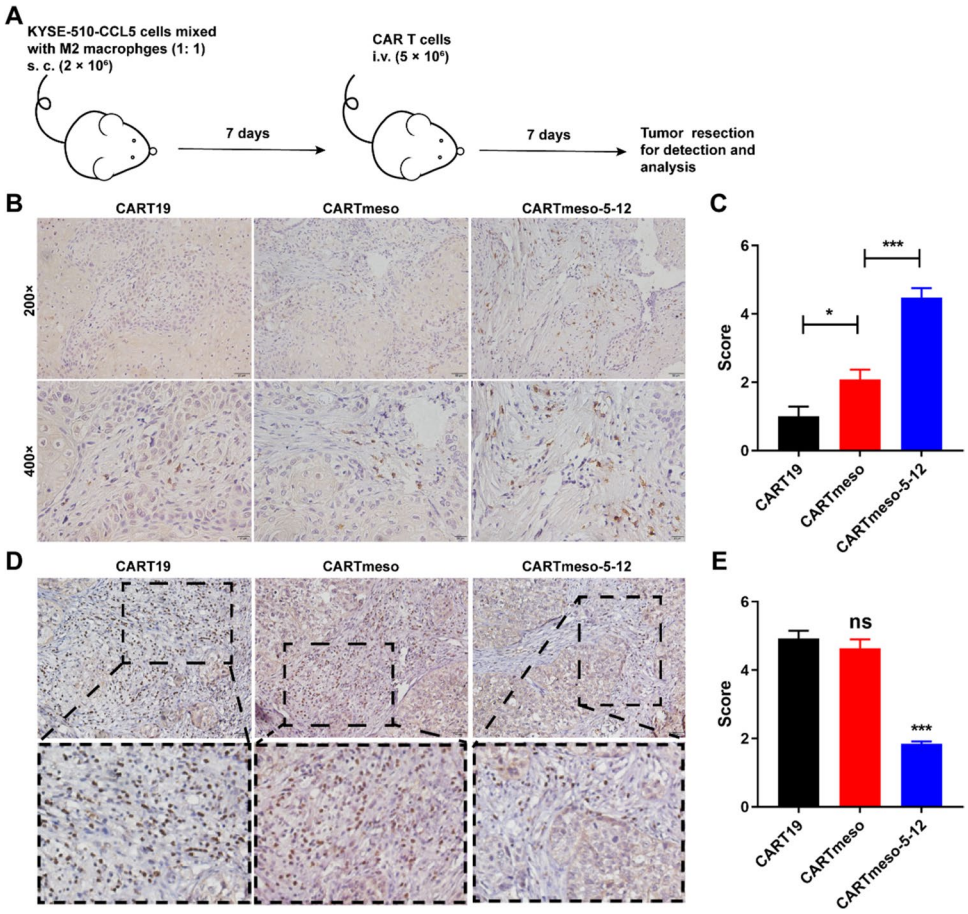

Fig. 5 Infiltration of tumor tissues treated with CAR T cells by both T cells and macrophages. **A** Experimental design for **B**–**E**. KYSE-510-CCL5 cells expressing luciferase mixed with M2 macrophages were injected s.c. into NOD/SCID mice. Mice received different CAR T cells infusion (i.v., 5×10^6) on the 7th day. Samples of mice were gathered for analysis on the 14th day. **B**, **C** Representative images and score of stained immunohistochemistry for human CD3 in tumor tissues. **D**, **E** Representative images and IHC score of CD163 immunohistochemical staining on tumor tissues from different groups of mice model. All data are represented as mean ± SEM. one-way ANOVA is used for statistical analysis. ns, not significant, $*p < 0.05$, $**p < 0.01$, $***P < 0.001$

(CCR5). Therefore, engineering CAR T cells with CCR5 is a viable and novel strategy for increasing their homing. The modified CARTmeso-CCR5 cells could improve the mobility without affecting the proliferation and cytotoxicity of CAR T cells.

Secondly, we analyzed the immune map by scRNA-seq results of lung cancer and ESCA data. Through the abundance composition of immune cells in the TME, we found that M2 macrophages were dominant in immunosuppressive cells. Cell interaction analysis further showed that TAMs mainly interacted with $CD8^+$ T cells to inhibit T cell function, indicating that remodeling macrophages can be used for the optimize tumor treatment. Some studies have suggested that increasing IL-12 concentrations in the TME can promote the transformation of macrophages from M2 to M1 cells and inhibit tumor growth [35]. Besides, IL-12 enhances T cell proliferation and cytotoxic activity, thereby promoting antitumor responses [36, 37]. Therefore, we constructed CAR T cells secreting IL-12 to surmount the inhibitory microenvironment and accelerate the antitumor ability of CAR T cells.

Therefore, we made CAR T cells simultaneously expressing both CCR5 and IL-12 (CARTmeso-5-12) to cope with various problems that may be encountered after CAR T cell infusion. Ali Hosseini. et al. compared the efficiency of four commonly used promoters (RPBSA, hPGK, CMV, and EF-1) and found that EF-1 promoter has the highest efficiency, followed by CMV promoter [38]. Therefore, CMV and EF-1 double-promoter construct was selected in our modified plasmid to ensure the stable expression of each gene. CCR5 facilitated the movement of CARTmeso-5-12 cells, which was conducive to their recruitment to the tumor site to fight tumors. Additionally, due to the addition of IL-12, CARTmeso-5-12 cells exhibited superior proliferative capacity and cytokine production, which could be beneficial for enhancing survival and antitumor effect. TAMs play a key role in tumor invasion and metastasis, and are mainly divided into tumor-suppressor M1 and tumor-promoting M2 [39, 40]. In vivo and in vitro results showed that CARTmeso-5-12 could transform M2 into M1 type and relieve immunosuppression and slow tumor growth. In this study, we mainly explored the function and efficacy of CARTmeso-5-12 in ESCA. In this study, we found that CCL5 and CCL4 were also high expression in other solid tumor tissues except ESCA, and that IL-12 function was non-tissue specific, suggesting that CARTmeso-5-12 cells have the potential to treat multiple solid tumors.

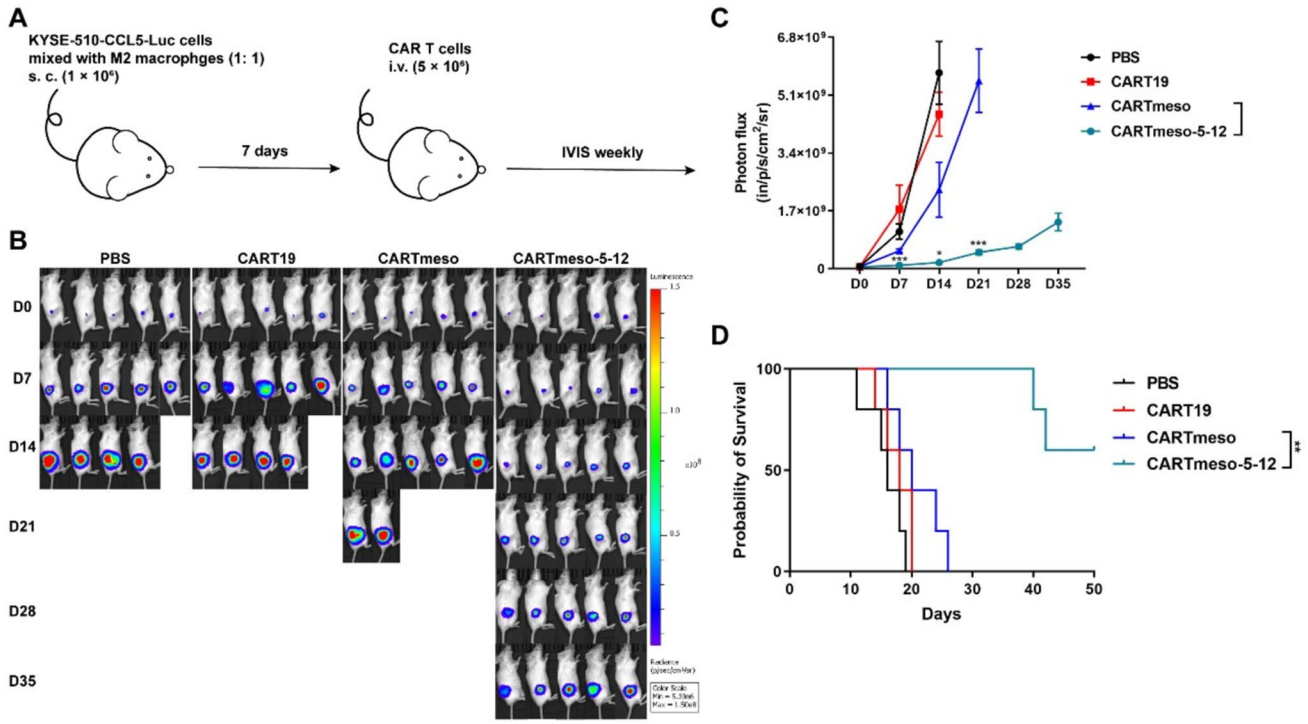

Fig. 6 CARTmeso-5-12 cells can better induce tumor elimination in vivo. **A** KYSE-510 cells expressing luciferase mixed macrophages were inoculated into NOD/SCID mice subcutaneously. On day 7, mice were treated with various CAR T cells. **B**, **C** Bioluminescence images of five representative mice in different groups were shown weekly to monitor tumor growth after adoptive therapies. Two-way ANOVA. **D** The survival curves of mice were performed. N = 5 mice/group, log-rank (Mantel-Cox) test. All data are represented as mean ± SEM. ns, not significant, $*p < 0.05$, $**p < 0.01$, $***P < 0.001$

Similarly, some researchers have designed CAR T cells to co-express IL-7 and CCL19/CCL21 to enhance the activity of CAR T cells and recruit endogenous immune cells [41, 42]. The difference is that in our study, CARTmeso-5-12 cells augmented their homing capacity. Furthermore, IL-12 expression not only elevated CAR T cell function, but also endowed the ability to polarize TAMs. Although CARTmeso-5-12 exhibit a powerful antitumor response, they may also bring side effects due to IL-12. This requires the introduction of an inducible expression system or a suicide gene to limit the systemic expression of IL-12.

In summary, we designed a novel CAR construct expressing the appropriate combination of CCR5 and IL-12 to address multiple barriers encountered by conventional CAR T cells in solid tumors. CARTmeso-5-12 cells can enhance their accumulation in tumor sites and the antitumor ability of CAR T cells and have the potential to reverse the immunosuppression of TME, providing a new strategy for the treatment of solid tumors. The enhanced efficacy in this study supplies preclinical evidence for subsequent clinical trials, with clinical translational significance.

Supplementary Information The online version contains supplementary material available at https://doi.org/10.1007/s00262-024-03909-w.

Author contributions Y.Z. planned and guided this research. Y.T., L.Z., Y. P., and Z.Z. conducted experiments. C.Y., C.S., F.L., and C.W. helped complete the experiment. Final manuscript read and approved by all authors.

Funding The work was supported by grants from Intergovernmental International Science and Technology Innovation Cooperation Project (Grant no. 2022YFE0141000), the National Natural Science Foundation of China (Grant no82272873), project of Central Leading Local Science and Technology Development of Henan Province (Z20221343036), Medical Science and Technology Project of Henan Province (SBGJ202101010).

Declarations

Conflicts of interest The authors declare no competing interests.

Data availability The data that support the findings of this study are available from the corresponding author upon reasonable request.

References

1. Albelda SM (2024) CAR T cell therapy for patients with solid tumours: key lessons to learn and unlearn. Nat Rev Clin Oncol 21(1):47–66
2. Shimabukuro-Vornhagen A, Böll B, Schellongowski P, Valade S, Metaxa V, Azoulay E, von Bergwelt-Baildon M (2022) Critical care management of chimeric antigen receptor T-cell therapy recipients. CA: Cancer J Clin 72(1):78–93
3. Cai F, Zhang J, Gao H, Shen H (2024) Tumor microenvironment and CAR-T cell immunotherapy in B-cell lymphoma. Eur J Haematol 112(2):223–235
4. Utkarsh K, Srivastava N, Kumar S, Khan A, Dagar G, Kumar M, Singh M, Haque S (2024) CAR-T cell therapy: a game-changer in cancer treatment and beyond. Clin Trans Oncol 26(6):1300–1318
5. Kolahi Azar H, Imanpour A, Rezaee H, Ezzatifar F, Zarei-Behjani Z, Rostami M, Azami M, Behestizadeh N, Rezaei N (2024) Mesenchymal stromal cells and CAR-T cells in regenerative medicine: The homing procedure and their effective parameters. Eur J Haematol 112(2):153–173
6. McNerney MP, Doiron KE, Ng TL, Chang TZ, Silver PA (2021) Theranostic cells: emerging clinical applications of synthetic biology. Nat Rev Genet 22(11):730–746
7. Rafiq S, Hackett CS, Brentjens RJ (2020) Engineering strategies to overcome the current roadblocks in CAR T cell therapy. Nat Rev Clin Oncol 17(3):147–167
8. Jin L, Tao H, Karachi A, Long Y, Hou AY, Na M, Dyson KA, Grippin AJ, Deleyrolle LP, Zhang W et al (2019) CXCR1- or CXCR2-modified CAR T cells co-opt IL-8 for maximal antitumor efficacy in solid tumors. Nat Commun 10(1):4016
9. Qu C, Zhang H, Cao H, Tang L, Mo H, Liu F, Zhang L, Yi Z, Long L, Yan L et al (2022) Tumor buster - where will the CAR-T cell therapy 'missile' go? Mol Cancer 21(1):201
10. Perera LP, Zhang M, Nakagawa M, Petrus MN, Maeda M, Kadin ME, Waldmann TA, Perera PY (2017) Chimeric antigen receptor modified T cells that target chemokine receptor CCR4 as a therapeutic modality for T-cell malignancies. Am J Hematol 92(9):892–901
11. Borlongan MC, Saha D, Wang H (2024) Tumor Microenvironment: A Niche for Cancer Stem Cell Immunotherapy. Stem Cell Rev Rep 20(1):3–24
12. Roselli E, Faramand R, Davila ML (2021) Insight into next-generation CAR therapeutics: designing CAR T cells to improve clinical outcomes. J Clin Invest. https://doi.org/10.1172/JCI142030
13. Khan MM, Li Y, Zhou Z, Ni A, Saiding Q, Qin D, Tao W, Chen W (2024) Macrophage-modulating nanomedicine for cancer immunotherapy. Nanoscale 16:7378–7386
14. Arnouk S, De Groof TWM, Van Ginderachter JA (2022) Imaging and therapeutic targeting of the tumor immune microenvironment with biologics. Adv Drug Deliv Rev 184:114239
15. Rodriguez-Garcia A, Lynn RC, Poussin M, Eiva MA, Shaw LC, O'Connor RS, Minutolo NG, Casado-Medrano V, Lopez G, Matsuyama T et al (2021) CAR-T cell-mediated depletion of immunosuppressive tumor-associated macrophages promotes endogenous antitumor immunity and augments adoptive immunotherapy. Nat Commun. https://doi.org/10.1038/s41467-021-20893-2
16. Gutiérrez-González A, Martínez-Moreno M, Samaniego R, Arellano-Sánchez N, Salinas-Muñoz L, Relloso M, Valeri A, Martínez-López J, Corbí ÁL, Hidalgo A et al (2016) Evaluation of the potential therapeutic benefits of macrophage reprogramming in multiple myeloma. Blood 128(18):2241–2252
17. Yang L, Dong Y, Li Y, Wang D, Liu S, Wang D, Gao Q, Ji S, Chen X, Lei Q et al (2019) IL-10 derived from M2 macrophage promotes cancer stemness via JAK1/STAT1/NF-κB/Notch1 pathway in non-small cell lung cancer. Int J Cancer 145(4):1099–1110
18. Liu JY, Li F, Wang LP, Chen XF, Wang D, Cao L, Ping Y, Zhao S, Li B, Thorne SH et al (2015) CTL- vs Treg lymphocyte-attracting chemokines, CCL4 and CCL20, are strong reciprocal predictive markers for survival of patients with oesophageal squamous cell carcinoma. Br J Cancer 113(5):747–755
19. Zheng Y, Chen Z, Han Y, Han L, Zou X, Zhou B, Hu R, Hao J, Bai S, Xiao H et al (2020) Immune suppressive landscape in the human esophageal squamous cell carcinoma microenvironment. Nat Commun 11(1):6268
20. Qian J, Olbrecht S, Boeckx B, Vos H, Laoui D, Etlioglu E, Wauters E, Pomella V, Verbandt S, Busschaert P et al (2020) A pan-cancer blueprint of the heterogeneous tumor microenvironment revealed by single-cell profiling. Cell Res 30(9):745–762
21. Wang Q, Cheng F, Ma TT, Xiong HY, Li ZW, Xie CL, Liu CY, Tu ZG (2016) Interleukin-12 inhibits the hepatocellular carcinoma growth by inducing macrophage polarization to the M1-like phenotype through downregulation of Stat-3. Mol Cell Biochem 415(1–2):157–168
22. Ma TT, Wu BT, Lin Y, Xiong HY, Wang Q, Li ZW, Cheng F, Tu ZG (2015) IL-12 could induce monocytic tumor cells directional differentiation. Mol Cell Biochem 402(1–2):157–169
23. Ping Y, Shan J, Qin H, Li F, Qu J, Guo R, Han D, Jing W, Liu Y, Liu J et al (2024) PD-1 signaling limits expression of phospholipid phosphatase 1 and promotes intratumoral CD8+ T cell ferroptosis. Immunity 57(9):2122
24. Kalbasi A, Ribas A (2020) Tumour-intrinsic resistance to immune checkpoint blockade. Nat Rev Immunol 20(1):25–39
25. Tian Y, Li Y, Shao Y, Zhang Y (2020) Gene modification strategies for next-generation CAR T cells against solid cancers. J Hematol Oncol 13(1):54
26. Hong M, Clubb JD, Chen YY (2020) Engineering CAR-T cells for next-generation cancer therapy. Cancer Cell 38(4):473–488
27. Moon EK, Carpenito C, Sun J, Wang LC, Kapoor V, Predina J, Powell DJ Jr, Riley JL, June CH, Albelda SM (2011) Expression of a functional CCR2 receptor enhances tumor localization and tumor eradication by retargeted human T cells expressing a mesothelin-specific chimeric antibody receptor. Clin Cancer Res Off J Am Assoc Cancer Res 17(14):4719–4730
28. Kim MY, Jayasinghe R, Devenport JM, Ritchey JK, Rettig MP, O'Neal J, Staser KW, Kennerly KM, Carter AJ, Gao F et al (2022) A long-acting interleukin-7, rhIL-7-hyFc, enhances CAR T cell expansion, persistence, and anti-tumor activity. Nat Commun 13(1):3296
29. Liu Y, Di S, Shi B, Zhang H, Wang Y, Wu X, Luo H, Wang H, Li Z, Jiang H (2019) Armored Inducible Expression of IL-12 Enhances Antitumor Activity of Glypican-3-Targeted Chimeric Antigen Receptor-Engineered T Cells in Hepatocellular Carcinoma. J Immunol (Baltimore, Md: 1950) 203(1):198–207
30. Gargett T, Ebert LM, Truong NTH, Kollis PM, Sedivakova K, Yu W, Yeo ECF, Wittwer NL, Gliddon BL, Tea MN et al (2022) GD2-targeting CAR-T cells enhanced by transgenic IL-15 expression are an effective and clinically feasible therapy for glioblastoma. J Immunotherapy Cancer 10(9):e005187
31. Ma X, Shou P, Smith C, Chen Y, Du H, Sun C, Porterfield Kren N, Michaud D, Ahn S, Vincent B et al (2020) Interleukin-23

engineering improves CAR T cell function in solid tumors. Nat Biotechnol 38(4):448–459
32. Zhang T, Tai Z, Miao F, Zhang X, Li J, Zhu Q, Wei H, Chen Z (2024) Adoptive cell therapy for solid tumors beyond CAR-T: current challenges and emerging therapeutic advances. J Controlled Release: Off J Controlled Release Soc 368:372–396
33. Albarrán V, San Román M, Pozas J, Chamorro J, Rosero DI, Guerrero P, Calvo JC, González C, García de Quevedo C, Pérez de Aguado P et al (2024) Adoptive T cell therapy for solid tumors: current landscape and future challenges. Front Immunol 15:1352805
34. Chen X, Zhao X, Mou X, Zhao J, Zhang Z, Zhang X, Huang J, Liu Y, Wang F, Zhang M et al (2024) PD-1-CD28-enhanced receptor and CD19 CAR-modified tumor-infiltrating T lymphocytes produce potential anti-tumor ability in solid tumors. Biomed Pharmacother 175:116800
35. Watkins SK, Egilmez NK, Suttles J, Stout RD (2007) IL-12 rapidly alters the functional profile of tumor-associated and tumor-infiltrating macrophages in vitro and in vivo. J Immunol (Baltimore Md: 1950) 178(3):1357–1362
36. Mirlekar B, Pylayeva-Gupta Y (2021) IL-12 family cytokines in cancer and immunotherapy. Cancers 13(2):167
37. Pawlowski KD, Duffy JT, Gottschalk S, Balyasnikova IV (2023) Cytokine modification of adoptive chimeric antigen receptor immunotherapy for glioblastoma. Cancers 15(24):5852
38. Ramos JW, Rad S (2020) M AH, Poudel A, Tan GMY, McLellan AD 2020 Promoter choice: Who should drive the CAR in T cells? PLoS ONE 15(7):e0232915
39. Kumari N, Choi SH (2022) Tumor-associated macrophages in cancer: recent advancements in cancer nanoimmunotherapies. J Exp Clin Cancer Res: CR 41(1):68
40. Yang Y, Guo J, Huang L (2020) Tackling TAMs for cancer immunotherapy: it's nano time. Trends Pharmacol Sci 41(10):701–714
41. Adachi K, Kano Y, Nagai T, Okuyama N, Sakoda Y, Tamada K (2018) IL-7 and CCL19 expression in CAR-T cells improves immune cell infiltration and CAR-T cell survival in the tumor. Nat Biotechnol 36(4):346–351
42. Luo H, Su J, Sun R, Sun Y, Wang Y, Dong Y, Shi B, Jiang H, Li Z (2020) Coexpression of IL7 and CCL21 increases efficacy of CAR-T cells in solid tumors without requiring preconditioned lymphodepletion. Clin Cancer Res: Off J Am Assoc Cancer Res 26(20):5494–5505